Monthly Notices
of the
ROYAL ASTRONOMICAL SOCIETY

Mon. Not. R. Astron. Soc. **422,** 2351–2356 (2012) doi:10.1111/j.1365-2966.2012.20786.x

Thermonuclear X-ray bursts from the 401-Hz accreting pulsar IGR J17498−2921: indication of burning in confined regions

Manoneeta Chakraborty⋆ and Sudip Bhattacharyya⋆

Department of Astronomy and Astrophysics, Tata Institute of Fundamental Research, Mumbai 400005, India

Accepted 2012 February 21. Received 2012 February 20; in original form 2012 January 2

ABSTRACT

We use the 2011 *Rossi X-ray Timing Explorer* (*RXTE*) Proportional Counter Array (PCA) data of the 401-Hz accreting pulsar and burster IGR J17498−2921 to perform timing analysis and time-resolved spectroscopy of 12 thermonuclear X-ray bursts. We confirm previously reported burst oscillations from this source with a much higher significance (8.8σ). We note that the bursts can be divided into three groups: big photospheric radius expansion (PRE) bursts are about 10 times more luminous than medium bursts, while the latter are about 10 times more luminous than small bursts. The PCA field of view of these observations contains several known bursters, and hence some of the observed bursts might not be from IGR J17498−2921. The oscillations during big bursts at the known pulsar frequency show that these bursts were definitely from IGR J17498−2921. We find that at least several of the other bursts were also likely originated from IGR J17498−2921. Spectral analysis reveals that the luminosity differences among various bursts are primarily due to differences in normalizations, and not temperatures, even when we consider the effects of colour factor. This shows burning on a fraction of the stellar surface for those small and medium bursts, which originated from IGR J17498−2921. The low values of the upper limits of burst oscillation amplitude for these bursts suggest a small angle between the spin axis and the magnetic axis. We find indications of the PRE nature of a medium burst, which likely originated from IGR J17498−2921. If true, then, to the best of our knowledge, this is the first time that two PRE bursts with a peak count rate ratio of as high as ≈12 have been detected from the same source.

Key words: methods: data analysis – stars: neutron – pulsars: general – X-rays: binaries – X-rays: bursts – X-rays: individual: IGR J17498−2921.

1 INTRODUCTION

Periodic intensity pulsations at the neutron star spin frequency, thermonuclear X-ray bursts and burst oscillations (brightness variations close to the spin frequency during the bursts) are observed from some neutron star low-mass X-ray binaries (LMXBs; Strohmayer & Bildsten 2006; Lamb et al. 2009). Modelling of these features can be useful to measure the neutron star parameters and to probe the strong gravity regime (e.g. Psaltis 2008; Bhattacharyya 2010). However, in order to use these features as tools, one needs to understand them sufficiently well. Although, their basic properties are well understood, there are several outstanding questions. For example, why some of the neutron star LMXBs are accreting pulsars (showing periodic pulsations), while others are not (e.g. Lamb et al. 2009; Özel 2009), what creates burning region asymmetry during decays of some thermonuclear bursts and gives rise to burst decay oscillations (Bhattacharyya 2010 and references therein), what causes the plausible confinement of the burning regions as indicated from timing analysis (e.g. Watts, Patruno & van der Klis 2008), etc. Accreting pulsars showing burst oscillations are the ideal sources to address these questions. In this paper, we report the results of detailed timing and time-resolved spectral analyses of the thermonuclear bursts from the *Rossi X-ray Timing Explorer* (*RXTE*) Proportional Counter Array (PCA) field of view (FoV) of the recently discovered accreting pulsar IGR J17498−2921 with neutron star spin frequency 400.99 Hz (Papitto et al. 2011). Linares et al. (2011) reported burst oscillations from this source. We confirm this feature with a much higher significance. We also show spectral indication of thermonuclear bursts from confined regions on the neutron star surface.

2 DATA ANALYSIS AND RESULTS

We analyse all the *RXTE* PCA data (32 obsIDs between August 13 and September 22; 146.496-ks exposure) of the 2011 outburst of the accreting 401-Hz pulsar IGR J17498−2921. 12 thermonuclear bursts are detected in the entire data (see Section 3 for discussions

⋆E-mail: manoneeta@tifr.res.in (MC); sudip@tifr.res.in (SB)

on thermonuclear origin, and on the sources which could give rise to these bursts). We carry out timing analysis and time-resolved spectroscopy, mostly using Good Xenon data files (∼0.95 μs time resolution), in order to study the nature of these bursts.

The properties of all the bursts are given in Table 1. The bursts can be divided into three groups, based on the pre-burst level subtracted peak count rates [$I_{\rm peak}$: counts per second per proportional counter unit (PCU)]: two big bursts with $I_{\rm peak} \approx 3600$–$3700$, three medium bursts with $I_{\rm peak} \approx 240$–300 and seven small bursts with $I_{\rm peak} \approx 45$–110 (see Fig. 1). However, this figure also shows that the shape and duration of bursts do not clearly change across the groups.

Now we search for oscillations from all the bursts in the entire PCA energy range (using all active PCUs). We start with the August 16 big burst for which burst oscillations were reported (see Section 1). The entire burst (above 5 per cent of the peak count rate) is divided into 33 ($=M$) segments of 1 s each. The Leahy normalized power spectra (Leahy et al. 1983; van der Klis 1989) from all of them are averaged to obtain a power spectrum of 1-Hz resolution; and a range of ±3 Hz from the known pulsar frequency (Section 1) is searched for a candidate peak. This is because the burst oscillation frequency does not shift from the neutron star spin frequency by more than 3 Hz (e.g. Strohmayer & Bildsten 2006). We find a candidate peak of ≈4.17 Leahy power at 401 Hz. The probability of obtaining such a high power in a single trial from the expected χ^2 noise distribution ($2M = 66$ degrees of freedom; van der Klis 1989) is $\approx 5.88 \times 10^{-7}$. Considering the number of trials to be 72 ($=6 \times 12$; six 1-Hz frequency bins are searched for each of the 12 bursts), the significance of detection is $\approx 4.1\sigma$ (estimated rms amplitude $\approx 4.6 \pm 0.2$ per cent). This suggests that a further and stronger detection would be required for confirmation of burst oscillations from IGR J17498−2921. Therefore, we perform a similar timing analysis for the August 20 big burst for $M = 33$. A candidate peak (≈7.04 Leahy power) appearing at 401 Hz has the single trial significance of $1-2.24 \times 10^{-20}$. Considering the number of trials to be 72 (as before), the significance of detection is $\approx 8.8\sigma$, which confirms burst oscillations from IGR J17498−2921 [see Fig. 2; note that this burst originated from IGR J17498−2921 (Section 3)]. If some of the 12 bursts were not originated from IGR J17498−2921 (Section 3), then the significance of oscillations from both the big bursts would be higher. The dynamic Z^2 power spectrum (Strohmayer & Markwardt 1999) of the August 20 big burst shows that the oscillations appear intermittently during burst decay and there is no significant frequency evolution (Fig. 3a). Fig. 3(b) shows the rms amplitude evolution during the August 20 big burst. However, burst oscillations are not detected from any medium or small burst. The 3σ upper limits of rms amplitude are 4.4, 5.0 and 5.1 per cent for all medium and small bursts combined (Fig. 2), for all medium bursts combined and for all small bursts combined, respectively.

Next we perform time-resolved spectroscopy of each burst after dividing them into time segments with sufficient counts. Note that each small burst has just one segment to maintain enough statistics. From each segment, we create an energy spectrum with dead time correction (van der Klis 1989), and a background spectrum from the pre-burst emission (Bhattacharyya & Strohmayer 2006; Galloway et al. 2008), considering only the top layers of all active PCUs. We fit each energy spectrum in 3−15 keV with a standard absorbed blackbody model (`phabs*bbodyrad` in XSPEC; Strohmayer & Bildsten 2006) for a fixed neutral hydrogen column density $N_{\rm H} = 2.87 \times 10^{22}\,{\rm cm}^{-2}$ (Torres et al. 2011), considering a systematic error of 1 per cent. The model fits the spectra well, with reduced $\chi^2 < 1.0$ (28 degrees of freedom) for ≈60 per cent spectra, and between 1.0 and 1.5 for almost all other spectra. The two big bursts show significant cooling in the decay portions, and the best-fitting blackbody temperature and normalization (defined in the caption of Fig. 3) evolve in a correlated way. The temperature profile of

Table 1. Properties of bursts from the 2011 *RXTE* PCA observations of IGR J17498−2921.

Serial no.	Observation start time[a]	Time in MJD[b]	Peak count rate[c] (count s^{-1})	τ[d] (s)	Temperature[e] (keV)	Normalization[f]	$\lvert R_1 - R_2\rvert/\sigma_{(R_1-R_2)}$[g]
1	2011-08-16T15:19:28	55789.64	3648.72 ± 61.32	6.07	$2.50^{+0.09}_{-0.09}$	$114.35^{+14.30}_{-12.98}$	
2	2011-08-19T12:11:28	55792.53	109.04 ± 14.90	4.13	$2.37^{+0.49}_{-0.37}$	$0.87^{+0.71}_{-0.41}$	1.37
3	2011-08-19T13:45:20	55792.58	291.08 ± 20.05	5.20	$2.77^{+0.35}_{-0.28}$	$5.81^{+2.42}_{-1.81}$	0.65
4	2011-08-19T15:19:28	55792.67	58.08 ± 12.96	4.17	$1.71^{+0.35}_{-0.28}$	$2.48^{+2.58}_{-1.29}$	1.03
5	2011-08-20T10:08:32	55793.43	76.69 ± 13.89	4.31	$1.93^{+0.34}_{-0.28}$	$1.69^{+1.38}_{-0.78}$	1.01
6	2011-08-20T10:08:32	55793.44	242.85 ± 18.98	4.12	$2.36^{+0.26}_{-0.22}$	$10.11^{+4.17}_{-3.07}$	6.89
7	2011-08-20T13:16:32	55793.59	3634.12 ± 61.20	7.05	$2.52^{+0.06}_{-0.06}$	$111.20^{+9.48}_{-8.82}$	1.72
8	2011-08-21T12:46:24	55794.57	273.42 ± 19.47	4.17	$2.28^{+0.28}_{-0.24}$	$8.85^{+4.16}_{-2.93}$	1.96
9	2011-08-29T08:47:28	55802.39	84.51 ± 13.31	3.30	$2.59^{+0.36}_{-0.29}$	$0.78^{+0.39}_{-0.27}$	0.88
10	2011-09-03T07:50:24	55807.34	60.40 ± 11.96	6.20	$2.04^{+0.30}_{-0.25}$	$1.49^{+0.95}_{-0.60}$	1.15
11	2011-09-08T05:49:20	55812.25	45.28 ± 11.06	6.06	$2.20^{+0.35}_{-0.28}$	$0.76^{+0.50}_{-0.32}$	0.26
12	2011-09-22T09:25:20	55826.41	83.99 ± 11.88	3.13	$1.75^{+0.51}_{-0.38}$	$1.08^{+1.83}_{-0.68}$	2.93

[a] The start time of the event data file containing the burst.
[b] The burst peak occurrence time in MJD.
[c] The pre-burst level subtracted burst peak count rate per PCU (PCU2), 1σ error is given.
[d] The exponential decay time for each burst.
[e] The best-fitting blackbody temperature in 3−15 keV, 90 per cent error is given (see Fig. 5).
[f] The best-fitting blackbody normalization in 3−15 keV, 90 per cent error is given (see Fig. 5; defined in the caption of Fig. 3).
[g] R_1: the ratio of observed total counts of a burst in the pair of PCUs; R_2: the expected value of R_1, if the burst were from IGR J17498−2921 (see Section 3). $\sigma_{(R_1-R_2)}$ is the estimated 1σ error in $R_1 - R_2$. Hence a lower value of $\lvert R_1 - R_2\rvert/\sigma_{(R_1-R_2)}$ implies a higher possibility for a burst to be originated from IGR J17498−2921. For burst 1, only one PCU was on.

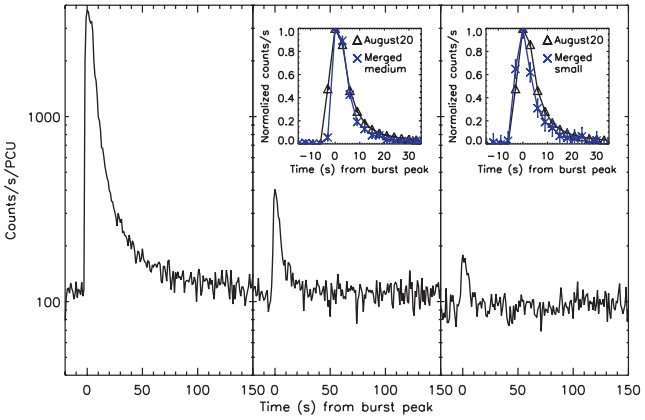

Figure 1. Example of each of the three types of bursts, big (left-hand panel; 2011 August 20), medium (middle panel; 2011 August 19) and small (right-hand panel; 2011 August 29), from the IGR J17498−2921 observations. Each *RXTE* PCA light curve has 1-s time binning. Note that the peak count rate of the big burst is about an order of magnitude larger than that of the medium burst, and the latter one is a few times larger than the peak count rate of the small burst. In the insets, normalized profile of the August 20 big burst is compared with that of three combined medium bursts, and that of seven combined small bursts, after aligning the peaks. These insets (with 3-s time bins) show, despite a large change of peak count rate from one burst to another, the shape/duration of the big, medium and small bursts are similar to each other (see Section 2).

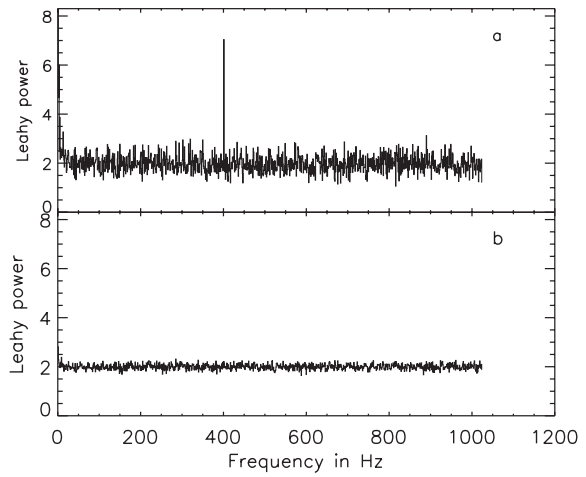

Figure 2. Leahy normalized power spectra from the *RXTE* PCA data of IGR J17498−2921. (a) Power spectra from 33 time segments (1 s each) during the big PRE burst (2011 August 20) are averaged without any further frequency rebinning. The strong peak at 401 Hz shows significant burst oscillations. (b) Same as (a) but the power spectra from all small and medium bursts are merged together. The power spectrum, which is an average of 331 power spectra, does not show burst oscillations (see Section 2).

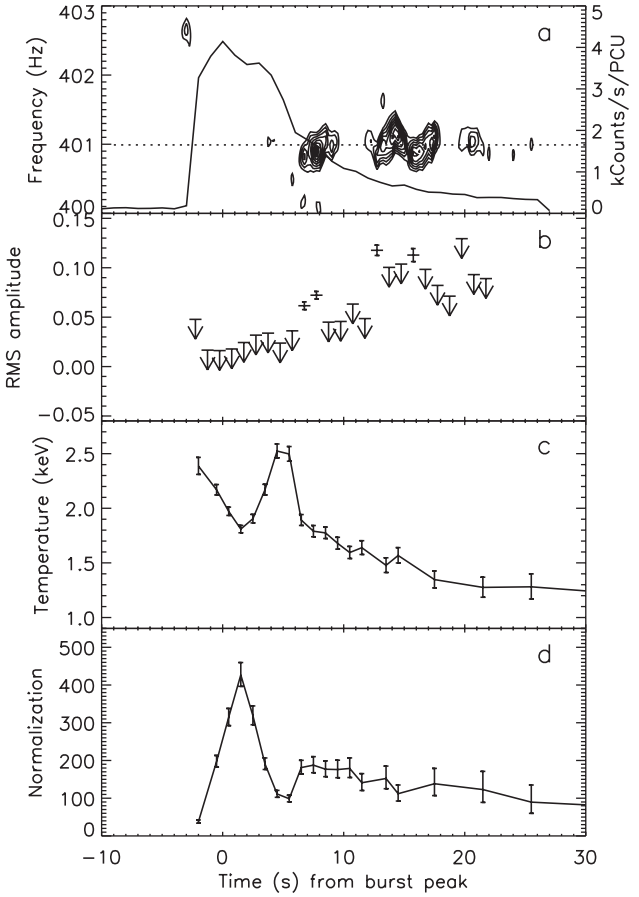

Figure 3. Properties of the big burst (2011 August 20) with oscillations from IGR J17498−2921. (a) *RXTE* PCA light curve (solid curve) and dynamic power spectrum (contours). The latter shows 30–99 per cent contours of the maximum power 37.8, using 2-s overlapping time bins with 0.25-s shift between two adjacent bins. These contours suggest the presence of an ≈401 Hz signal with no significant frequency evolution. The dotted horizontal line shows the pulsar frequency (see Section 2). (b) Fractional rms amplitudes in 1-s bins during the burst. 1σ error bars are given for 3σ significant four amplitudes (6.24 ± 0.39, 7.14 ± 0.38, 11.53 ± 0.53 and 11.23 ± 0.66 per cent), and 3σ upper limits are given for the rest (see Section 2). (c) The evolution of the best-fitting (in 3−15 keV) blackbody temperature (with 90 per cent errors) of the burst (see Section 2). The rise of the temperature is not seen because of the somewhat large time bin. (d) The evolution of the best-fitting (in 3−15 keV) blackbody normalization (with 90 per cent errors) of the burst. This normalization is proportional to the burning area, and is defined as $R_{\rm km}^2/D_{10}^2$, where $R_{\rm km}$ is the neutron star radius in km when the entire surface emits and D_{10} is the distance to the source in the unit of 10 kpc. The specific correlation between the temperature and the normalization shows that this is a PRE burst (see Section 2).

each big burst shows two peaks, while a normalization peak coincides with the temperature minimum between two peaks (see Fig. 3 for the August 20 burst). This is a clear signature of a photospheric radius expansion (PRE) burst (e.g. Galloway et al. 2008; see also Chakraborty & Bhattacharyya 2011b; Linares et al. 2011). The medium bursts also show a cooling trend during decay (e.g. Fig. 4). This figure also shows a somewhat correlation between the best-fitting blackbody temperature and normalization, which is indicative of the PRE nature of the August 19 medium burst (see Section 3 for a discussion). We find that the best-fitting blackbody temperatures of all the bursts are consistent with each other (see Fig. 5 and Section 3). However, the corresponding best-fitting normalizations are correlated with the burst fluence (integrated energy) values, and both parameters increase roughly by two orders of magnitude from small to big bursts (see Fig. 5). Finally, in order to track the temperature evolution in a model-independent way, we plot the burst colour (ratio of pre-burst level subtracted count rate above 6.14 keV to that below 6.14 keV) with time (Fig. 6). This figure supports the finding that the temperatures of all the bursts are consistent with each other and also shows a cooling trend during the decay of small bursts. A dip in colour (Fig. 6) near the peak count rate supports a plausible PRE nature of the August 19 medium burst (see above).

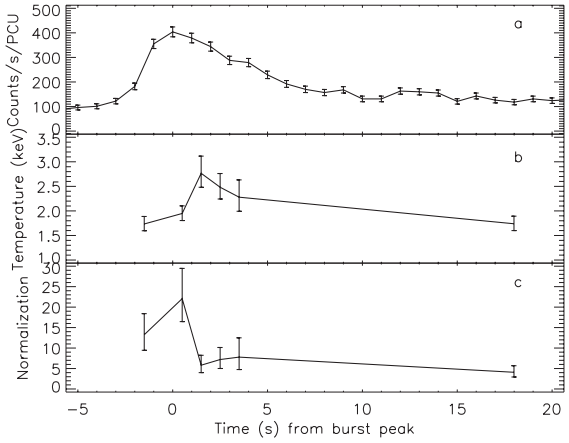

Figure 4. Parameter evolution for a medium burst (2011 August 19) from an IGR J17498−2921 observation. (a) Count rate evolution with 1-s time bins. (b) The evolution of the best-fitting (in 3−15 keV) blackbody temperature (with 90 per cent errors) of the burst. (c) The evolution of the best-fitting (in 3−15 keV) blackbody normalization (defined in the caption of Fig. 3; with 90 per cent errors) of the burst. The specific correlation between the temperature and the normalization (especially when compared with panels c and d of Fig. 3) indicates PRE, although the first temperature peak is not visible (see Sections 2 and 3).

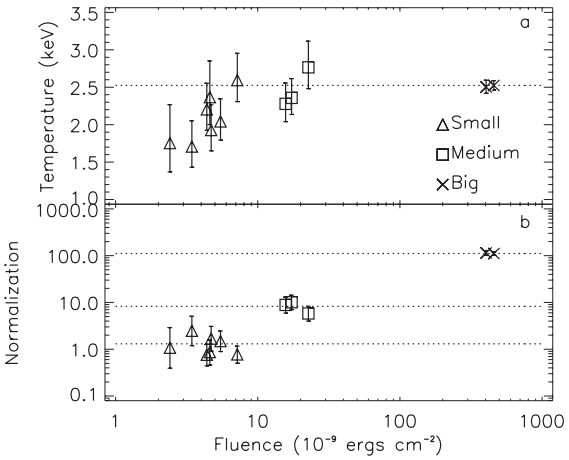

Figure 5. Best-fitting blackbody temperature (a) and normalization (b; defined in the caption of Fig. 3) in 3−15 keV as functions of the burst fluence for all *RXTE* PCA bursts from IGR J17498−2921 observations. Note that for each small burst, only one spectrum for the entire burst duration is fitted and the corresponding temperature and normalization are plotted. For each medium and big burst, the maximum temperature reached during the burst and its corresponding normalization are plotted. Cross signs: big bursts; square signs: medium bursts; triangle signs: small bursts. 90 per cent error bars are given. (a) The dotted horizontal line goes through the big burst (2011 August 20) temperature. (b) The dotted horizontal lines from top to bottom go through the big burst (2011 August 20) normalization, mean normalization of medium bursts and mean normalization of small bursts, respectively. This figure shows that, while the temperatures of all the bursts are similar to each other, the normalization (and hence the burning area) is correlated with the burst fluence, and it increases from small to big bursts by about two orders of magnitude (see Section 2).

3 DISCUSSION AND CONCLUSIONS

We discuss the implications of our results in this section. Let us first show that all the 12 bursts are thermonuclear bursts. The sharp rise and slow decay of intensity, acceptable fitting of burst spectra with a

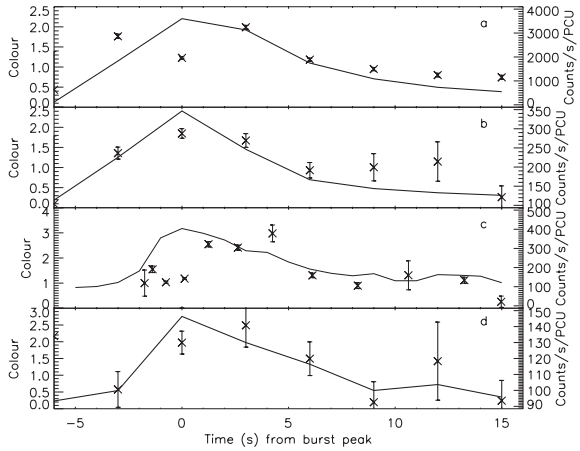

Figure 6. The colour (cross sign with 1σ error; ratio of the persistent-subtracted count rate above 6.14 keV to that below 6.14 keV) and count rate (solid curve) evolution during the bursts from the *RXTE* PCA observations of IGR J17498−2921. (a) Big burst (2011 August 20). (b) Three medium bursts averaged. (c) The brightest medium burst (August 19). (d) Seven small bursts averaged. Burst peaks are made aligned for averaging. This figure shows that (1) the maximum values of colour for big, medium and small bursts are similar to each other; (2) there is a decreasing trend of colour during the decays of big, medium and small bursts; and (3) a dip in colour near the peak count rate of the brightest medium burst (August 19) is consistent with a plausible PRE nature (see Section 2). However, we note that such a dip is not seen in the average profiles (panels b and d).

blackbody model, cooling during burst decay and detection of burst oscillations leave no doubt that the big bursts are of thermonuclear origin. The first three properties are also true for medium and small bursts. The very similar shape and duration of all the burst profiles argues that if big bursts are thermonuclear, then others from the same source are thermonuclear bursts too. Besides these are not repetitive bursts and hence are not accretion-powered type II bursts (e.g. Chakraborty & Bhattacharyya 2011a). These establish that all the 12 bursts are thermonuclear.

The PCA FoV of IGR J17498−2921 contains five additional known thermonuclear X-ray bursters: XTE J1747−274 (or IGR J17473−2721), SAX J1750.8−2900, SAX J1747.0−2853, 1A 1742−289 (or AX J1745.6−2901) and SLX 1744−299/300. This brings the question whether some or all of the 12 detected bursts (Section 2) were not from IGR J17498−2921. The two big bursts showed oscillations at the known pulsar frequency of 401 Hz, and hence they were definitely from IGR J17498−2921. But which sources gave rise to the medium and small bursts? The first four of the five above-mentioned additional bursters are transients, and none of them reportedly was in outburst during the outburst of IGR J17498–2921 [otherwise, the scanning programmes of satellites, such as *INTEGRAL* (e.g. Gibaud et al. 2011), would detect such an outburst]. Since a thermonuclear burst from the quiescent phase of a transient is very rare (e.g. Kuulkers, in't Zand & Lasota 2009), it is unlikely that the medium and small bursts originated from one of the four known transient bursters, or any other heretofore unknown transient burster in quiescence in the FoV. Here we consider that the medium and small bursts have originated from IGR J17498−2921 and/or from the persistent burster SLX 1744−299/300 though there still remains a small chance that a low-intensity outburst (missed by X-ray satellites) of a transient at the edge of the FoV could give rise to one or more of these bursts. Three bursts were previously observed with PCA from SLX 1744−299/300 (Galloway et al. 2008). We find that the shape and duration of these bursts were similar to

those of our 12 bursts. The peak count rates (when corrected for the off-axis position of the source) of all these SLX 1744−299/300 bursts are less than those of our medium bursts but greater than those of our small bursts. Therefore, the shape, duration and peak count rate do not reveal whether our small and medium bursts were from SLX 1744−299/300 or IGR J17498−2921. Table 3 of Galloway et al. (2008) shows that the occurrence of SLX 1744−299/300 bursts per hour was 0.037 for 290 ks of PCA observation. If all our medium and small bursts had originated from SLX 1744−299/300, then the burst rate of this source would be $0.246\,h^{-1}$, which is about seven times larger than the known burst rate ($0.037\,h^{-1}$). Even if only the small bursts had come from SLX 1744−299/300, its burst rate would be about five times larger than the known rate. These suggest that not all the medium and small bursts may have originated from SLX 1744−299/300, which implies that at least some of these bursts were from IGR J17498−2921. In order to know whether this is indeed the case, we attempt to find out if the angular location of a burst is consistent with that of IGR J17498−2921. For this, we exploit the fact that the five PCUs are not perfectly aligned (Jahoda et al. 2006), and hence the ratio of observed count rates in a pair of PCUs depends upon the position of the source within the FoV (Galloway et al. 2008). Two PCUs were on for each of the bursts, except for the August 16 big burst (one PCU). Therefore, for each of the 11 bursts, we compute the ratio (R_1, with an error) of observed total counts (pre-burst level subtracted and dead time corrected) in the pair of PCUs. For the PCA observations of IGR J17498−2921, this source was almost (within a few arcsec) at the centre of the FoV. Therefore, if an R_1 value is consistent with the expected value for the centre of PCA FoV, then the corresponding burst likely originated from IGR J17498−2921. In order to find out these expected values, we consider several bursts in PCA observations from two other sources (4U 1636−536 and 4U 1608−52), which were at the centre of PCA FoV, and for each of which there is no known burster in the PCA FoV. For these sources and for each pair of PCUs, we compute a mean burst count ratio (R_2, with an error) in the same way we compute R_1. These R_2 values are the expected ratio values for the centre of PCA FoV. We compare an R_1 value with the R_2 value for the same PCU pair. For each of the 11 bursts, Table 1 gives the difference between R_1 and R_2 in the unit of the estimated error in this difference. A smaller value of this difference implies a higher possibility for a burst to be originated from IGR J17498−2921. For example, this difference is less than 1 for the brightest medium burst [August 19; for which a plausible PRE nature is seen (Section 2)] and two small bursts, implying that these bursts were likely to be originated from IGR J17498−2921.

Based on the above discussion and Table 1, in the rest of this section we assume that at least one medium burst and at least one small burst were originated from IGR J17498−2921. We now ask the question what made some bursts from IGR J17498−2921 so energetic, while one or more other bursts were so weak? Was it because of burning of different chemical compositions in different accretion rate regimes (Strohmayer & Bildsten 2006 and references therein)? We find that this is very improbable because (1) the shape and duration of all the burst profiles are similar, indicating the burning of similar compositions and (2) the burst fluence is not correlated with the persistent intensity. For example, the persistent intensities before one of the August 19 small bursts and before the August 29 small burst are, respectively, slightly higher and slightly lower than the persistent intensity before the August 20 big burst. Hence we try to find if the increase of the fluence from small to big bursts for IGR J17498−2921 is due to the blackbody temperature increase or due to the burning area ($\propto$ blackbody normalization) increase. Figs 3(c), 4(b), 5(a) and 6 show that the best-fitting temperatures of one burst are consistent with those of others. In Fig. 5(a), the temperatures of small bursts are somewhat systematically less than those of medium and big bursts; but this is because the former temperatures are average values during burst profiles, while the latter temperatures are the maximum values during burst profiles. Note that such a maximum temperature value for a big burst is for the second temperature peak, which corresponds to the touchdown point (i.e. settling of the photosphere on the stellar surface after expansion). Unlike the temperature, the normalization, which is proportional to the burning area (see caption of Fig. 3), increases significantly with fluence (Fig. 5b; Section 2). This strongly suggests that the burning area increases from small to big bursts for IGR J17498−2921, while the other parameters, including the temperature and composition, remain roughly unchanged. If this is true, then each burst from IGR J17498−2921 should be similarly strong within its confinement (burning area), and hence, even the small and medium bursts from this source could have local photosphere expansion. However, for a smaller burst, a signature of such expansion (discussed in Section 2) is washed away due to the large time bins required to gather sufficient counts for spectral analysis. Nevertheless, such a signature appears for the brightest medium burst (Figs 4b and c; Section 2), which is likely to be originated from IGR J17498−2921 (see Table 1, burst 3). Although, a temperature peak before the peak intensity is not there, the following properties indicate the photosphere expansion: (1) normalization evolution is very similar to that of the big bursts (compare Fig. 3d with Fig. 4c), (2) intensity peak corresponds to the normalization peak and a low temperature and (3) a temperature peak (corresponding to a low normalization) appears after the intensity peak. Moreover, an observed dip in colour near the burst intensity peak (Fig. 6c) suggests a similar dip in temperature (undetected plausibly due to large time bin as mentioned above), and hence a plausible temperature peak before the peak intensity. However, a conclusion about the PRE nature of this burst has to be made cautiously because (1) a temperature peak before the peak intensity is not significantly detected and (2) the normalization value following the maximum is not lower with at least 4σ significance (as considered by Galloway et al. 2008). If this medium burst is really a PRE burst, then, to the best of our knowledge, this is the first time that two PRE bursts with a peak count rate ratio of as high as $\approx$12 have been detected from the same source (e.g. Galloway et al. 2006). This makes the standard method of source distance measurement using PRE bursts (e.g. Kuulkers et al. 2003) somewhat less reliable, at least for pulsars. All the bursts from IGR J17498−2921 were likely helium-rich because of their high temperatures, somewhat short durations and the PRE nature (for at least the two big bursts; see e.g. Galloway & Cumming 2006; Galloway et al. 2008).

The blackbody normalization values for small and medium bursts (Fig. 5b) imply burning areas much smaller than any realistic neutron star surface area (e.g. for a stellar radius of 8–20 km), implying burning in confined regions. Note that these normalization values are estimated assuming a source distance of 10 kpc (see caption of Fig. 3). If the distance is less (e.g. 7.6 kpc for IGR J17498−2921 as reported by Linares et al. 2011), the intrinsic normalization values will be smaller (implying even smaller burning areas) by a factor same for all the bursts from a given source. A correction due to the surface gravitational redshift $1 + z$ (Sztajno et al. 1985) will make the intrinsic normalization values further smaller by another factor $(1 + z)^2$, which is same for all the bursts from a given source.

The absorption and scattering in the neutron star atmosphere make the observed temperature higher (relative to the intrinsic

temperature) by a factor f, and the observed normalization lower (relative to the intrinsic normalization) by a factor f^4, where f is the colour factor (Sztajno et al. 1985; Majczyna et al. 2005; Bhattacharyya, Miller & Galloway 2010; Suleimanov, Poutanen & Werner 2011). Does this mean that our conclusion about burning in confined regions for IGR J17498−2921 is not robust? In order to find out, let us examine, if the burning areas of the big bursts cover the entire neutron star surface, then, whether the burning area of a medium burst from IGR J17498−2921 can also cover the entire surface. How could this happen? Suppose, the intrinsic temperature of the medium burst is smaller than that of big bursts, and f increases with the decrease of temperature to make the observed temperature of the medium and big bursts similar. Then the ratio of a big burst intrinsic normalization to the medium burst intrinsic normalization will be lower (by a factor, say, g) than the ratio of a big burst observed normalization to a medium burst observed normalization (the observed normalizations are given in Fig. 5b). If $g \sim 10$, then the burning areas of the medium bursts could be similar to those of big bursts (Fig. 5b). However, considering the relevant extreme f values (1.64, 1.22) from the tables of Majczyna et al. (2005), $g < 3.3\,(= [1.64/1.22]^4)$. Therefore, even if we consider the maximum possible value (i.e. the entire surface) for a big burst burning area, a medium burst (from IGR J17498−2921) burning area cannot be more than ∼35 per cent of the stellar surface, even after considering the effects of colour factor. With the same arguments, a small burst (from IGR J17498−2921) burning area will be even smaller. This shows that our conclusion about burning in confined regions is robust. Finally, we note that the observed burning areas of some of the bursts may be small due to obscuration (for example, if the observer is close to one spinning pole and burning regions are close to the other); but even for this, the burning has to happen in confined regions. Even if all the medium and small bursts were from SLX 1744−299/300, the difference in normalization values between these two sets of bursts would indicate confined burning for small bursts for this source. However, we note that the confined burning could be more easily explained for IGR J17498−2921 (than for SLX 1744−299/300), which is a known pulsar, and hence likely to have a higher neutron star magnetic field (see the following paragraph).

Our results support a prediction of Bildsten (1993) that the weaker bursts are from small fractions of the neutron stars. The low values of the upper limits of burst oscillation fractional rms amplitude for small and medium bursts (see Section 2) suggest that the burning regions for IGR J17498−2921 were close to a spinning pole (assuming a hotspot model; Lamb et al. 2009). Hence, a reasonable assumption that the thermonuclear burning happens close to the magnetic pole(s) (as the accreted matter is channelled to these poles for a pulsar) implies that the spin axis and the magnetic axis of this pulsar are close to each other. This supports the Lamb et al. (2009) model of accreting millisecond X-ray pulsars. What gave rise to oscillations during the decays of big bursts? If the burning covered the entire neutron star surface, then the oscillations could be due to a complex asymmetric brightness pattern, caused by Rossby waves (or r modes) in the surface layers, shear instabilities, etc. (e.g. Cumming 2005; Heyl 2005; Lee & Strohmayer 2005; Piro & Bildsten 2006). Finally, what confined the burning region, and why did the burning area change from burst to burst? Detailed theoretical and numerical studies are required to answer these questions. The confined burning could be due to the magnetic field near the magnetic pole (but see Watts et al. 2008), magnetic field locally enhanced by the convection during thermonuclear flame spreading (e.g. Spitkovsky, Levin & Ushomirsky 2002), magnetic structure (e.g. belt) on the neutron star surfaces (e.g. Payne & Melatos 2006), higher local temperature (sufficient for ignition) near the magnetic poles, while ignition condition is not reached at rest of the stellar surface (Watts et al. 2008), or something else. Whatever be the reason, the indication of burning in confined regions reported in this paper may have significant impact in understanding the accreting pulsars, burst oscillations, burst ignition conditions, surface magnetic field structure and its interaction with flame spreading, etc. (see also Section 1).

ACKNOWLEDGMENT

This research has made use of data obtained from the High Energy Astrophysics Science Archive Research Center (HEASARC), provided by NASA's Goddard Space Flight Center. We thank an anonymous referee for very constructive and useful comments, which improved the paper.

REFERENCES

Bhattacharyya S., 2010, Advances Space Res., 45, 949
Bhattacharyya S., Strohmayer T. E., 2006, ApJ, 641, L53
Bhattacharyya S., Miller M. C., Galloway D. K., 2010, MNRAS, 401, 2
Bildsten L., 1993, ApJ, 418, L21
Chakraborty M., Bhattacharyya S., 2011a, ApJ, 730, L23
Chakraborty M., Bhattacharyya S., 2011b, Astron. Telegram, 3643, 1
Cumming A., 2005, ApJ, 630, 441
Galloway D. K., Cumming A., 2006, ApJ, 652, 559
Galloway D. K., Psaltis D., Muno M. P., Chakrabarty D., 2006, ApJ, 639, 1033
Galloway D. K., Muno M. P., Hartman J. M., Psaltis D., Chakrabarty D., 2008, ApJS, 179, 360
Gibaud L. et al., 2011, Astron. Telegram, 3551, 1
Heyl J. S., 2005, MNRAS, 361, 504
Jahoda K., Markwardt C. B., Radeva Y., Rots A. H., Stark M. J., Swank J. H., Strohmayer T. E., Zhang W., 2006, ApJS, 163, 401
Kuulkers E., den Hartog P. R., in't Zand J. J. M., Verbunt F. W. M., Harris W. E., Cocchi M., 2003, A&A, 399, 663
Kuulkers E., in't Zand J. J. M., Lasota J.-P., 2009, A&A, 503, 889
Lamb F. K., Boutloukos S., van Wassenhove S., Chamberlain R. T., Lo K. H., Clare A., Yu W., Miller M. C., 2009, ApJ, 706, 417
Leahy D. A., Darbro W., Elsner R. F., Weisskopf M. C., Sutherland P. G., Kahn S., Grindlay J. E., 1983, ApJ, 266, 160
Lee U., Strohmayer T. E., 2005, MNRAS, 361, 659
Linares M. et al., 2011, Astron. Telegram, 3568, 1
Majczyna A., Madej J., Joss P. C., Różańska A., 2005, A&A, 430, 643
Özel F., 2009, ApJ, 691, 1678
Papitto A. et al., 2011, A&A, 535, L4
Payne D. J. B., Melatos A., 2006, ApJ, 652, 597
Piro A. L., Bildsten L., 2006, ApJ, 638, 968
Psaltis D., 2008, Living Rev. Relativ., 11, 9
Spitkovsky A., Levin Y., Ushomirsky G., 2002, ApJ, 566, 1018
Strohmayer T. E., Bildsten L., 2006, in Lewin W. H. G., van der Klis M., eds, Cambridge Astrophys. Ser. Vol. 39, Compact Stellar X-ray Sources. Cambridge Univ. Press, Cambridge, p. 113
Strohmayer T. E., Markwardt C. B., 1999, ApJ, 516, L81
Suleimanov V., Poutanen J., Werner K., 2011, A&A, 527, A139
Sztajno M., van Paradijs J., Lewin W. H. G., Trümper J., Stollman G., Pietsch W., van der Klis M., 1985, ApJ, 299, 487
Torres M. A. P., Madej O., Jonker P. G., Steeghs D., Greiss S., Morrell N., Roth M., 2011, Astron. Telegram, 3638, 1
van der Klis M., 1989, in Ögelman H., van den Heuvel E. P. J., eds, Timing Neutron Stars. Kluwer, New York, p. 27
Watts A. L., Patruno A., van der Klis M., 2008, ApJ, 688, L37

This paper has been typeset from a TEX/LATEX file prepared by the author.